International Journal of Bifurcation and Chaos
© World Scientific Publishing Company

Different types of attractors in the Three Body Problem perturbed by dissipative terms

John D. Hadjidemetriou
Department of Physics, University of Thessaloniki, Thessaloniki, Greece
hadjidem@auth.gr.

George Voyatzis
Department of Physics, University of Thessaloniki, Thessaloniki, Greece
voyatzis@auth.gr

Received (to be inserted by publisher)

We study the evolution of a conservative dynamical system with three degrees of freedom, where small non conservative terms are added. The conservative part is a Hamiltonian system, describing the motion of a planetary system consisting of a star, with a large mass, and of two planets, with small but not negligible masses, that interact gravitationally. This is a special case of the three body problem, which is non integrable. We show that the evolution of the system follows the topology of the conservative part. This topology is critically determined by the families of periodic orbits and their stability. The evolution of the complete system follows the families of the conservative part and is finally trapped in the resonant orbits of the Hamiltonian system, in different types of attractors: Chaotic attractors, limit cycles or fixed points.

Keywords: periodic orbits, resonance, dissipation, attractors.

1. Introduction

It is known that attractors cannot appear in a conservative system, because the volume in phase space is conserved. On the contrary, different types of attractors appear in a dissipative system. This is also the case when Hamiltonian systems are perturbed by terms which destroy the conservative nature of the system.

In the present work we study the evolution of a conservative, Hamiltonian, system where small non conservative terms are added as a perturbation. Particularly we consider a planetary system consisting of the star (with a large mass) and two planets, with small but non negligible masses, that interact gravitationally. This is the general three body problem of planetary type, which is a non integrable Hamiltonian system. We assume the planar case, i.e. all bodies move in the same plane (see Fig. 1a). If we assume that the planetary system is not yet fully developed and a protoplanetary nebula exists, then the motion of the planets is affected by the drag which is due to the interaction between the planets and the protoplanetary nebula. Such a dissipation effect lasts until this nebula is dissolved and the system takes its final form. This kind of study has been made in order to explain the large eccentricities, or the very close proximity of the planets, and the resonance trapping in several observed extrasolar planetary systems ([Beaugé and Ferraz-Mello, 1993], [Beaugé et al., 2006], [Ferraz-Mello et al., 2003], [Gomes , 1996], [Morbidelli et al., 2007], [Nelson and Papaloizou, 2003a], [Nelson and Papaloizou, 2003b], [Papaloizou, 2003], [Hadjidemetriou and Voyatzis, 2010]).

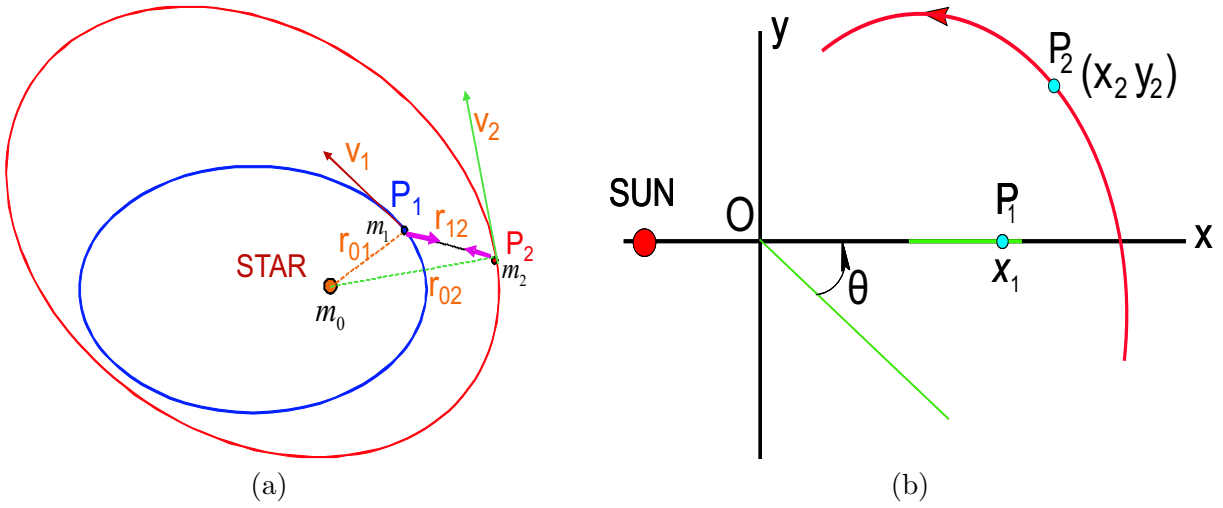

(a) (b)

Fig. 1. (a) The two planets in elliptic orbits that interact gravitationally. (b) The rotating frame xOy. The angle θ is ignorable.

In section 2 we introduce our model and discuss the dynamics of the Hamiltonian system, namely the planar three body problem in a rotating frame. We also determine the families of periodic orbits of the system which play an essential role in our study. In section 3 we present the results of our numerical simulations and illustrate the stages of a resonance trapping due to the dissipation terms. Finally, in section 4, we discuss the main points of our study.

Dissipative Hamiltonian systems are not used only as models for astronomical problems, but can find many applications for system stabilization and control (see e.g. [Crouch and van der Schaft, 1987]).

2. The model and the families of periodic orbits

2.1. *The model in the inertial frame of reference.*

We consider the star S, with mass m_0 and the two planets P_1 and P_2, with masses m_1 and m_2, respectively, moving in the same plane, in an inertial frame where the center of mass of the system is fixed at the origin of a coordinate system $X\Omega Y$. We have four degrees of freedom, since the position of the system is determined by the coordinates X_1, Y_1 and X_2, Y_2 of the two planets (the position of the star is obtained from the fact that the center of mass is at Ω).

It is assumed that the nebula, which introduces the drag, rotates with Keplerian circular velocity (at each radius r) and the non conservative force is a linear drag law proportional to the relative velocity of the planets with respect to the nebula:

$$\vec{R} = -10^{-n}(\vec{v} - \vec{v}_c), \tag{1}$$

where $\vec{v}$ is the velocity of the planet and $\vec{v}_c$ is the circular velocity of the nebula, given by

$$\vec{v}_c = \sqrt{\frac{Gm}{r}}\vec{e}_\theta. \tag{2}$$

In fact, the purely dissipative force in Eq. (1) is the component $-10^{-n}(\vec{v})$ and the component $-10^{-n}(-\vec{v}_c)$ is a forcing force, due to the rotation of the nebula, which is imposed to the system. This means that the nonconservative force given by Eq. (1) may be either positive or negative, depending on the relative velocity of the planet with respect to the circular velocity at that point. This type of drag force has been used by [Beaugé et al., 2006], with a range of the values of the exponent n in Eq. (1) between 4 and 11. In the following we shall call the force given by Eq. (1) *dissipative*, with the meaning that the dissipation may be either positive or negative, as explained above.

The differential equations of motion in the inertial frame are

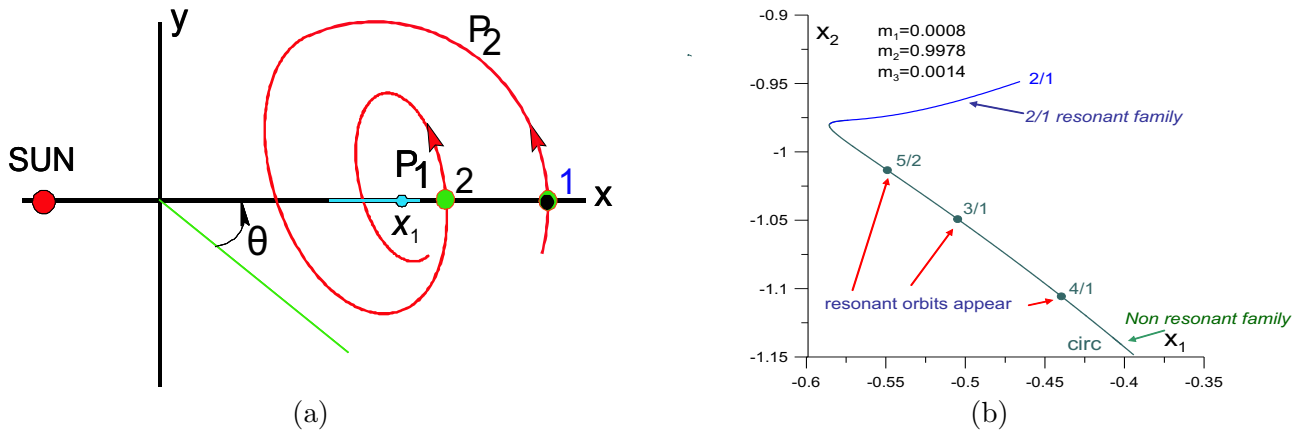

Fig. 2. (a) The Poincaré map on the surface of section $y_2 = 0$, $\dot{y} > 0$. (b) The circular family of periodic orbits (green), until the bifurcation to the 2/1 resonant elliptic family of periodic orbits (blue). Along the circular family there appear resonant orbits.

$$\begin{aligned}
\ddot{x}_1 &= -m_0\frac{x_1 - x_0}{r_{01}^3} - m_2\frac{x_1 - x_2}{r_{12}^3} + \frac{R_{1x}}{m_1},\\
\ddot{y}_1 &= -m_0\frac{y_1 - y_0}{r_{01}^3} - m_2\frac{y_1 - y_2}{r_{12}^3} + \frac{R_{1y}}{m_1},\\
\ddot{x}_2 &= -m_0\frac{x_2 - x_0}{r_{02}^3} - m_1\frac{x_2 - x_1}{r_{12}^3} + \frac{R_{2x}}{m_2},\\
\ddot{y}_2 &= -m_0\frac{y_2 - y_0}{r_{02}^3} - m_1\frac{y_2 - y_1}{r_{12}^3} + \frac{R_{2y}}{m_2},
\end{aligned} \tag{3}$$

and include the gravitational interaction between the bodies and also the dissipative force acting on each planet. r_{01}, r_{02} and r_{12} are the distances between S and P_1, S and P_2 and P_1 and P_2, respectively. (R_{1x}, R_{1y}) and (R_{2x}, R_{2y}) are the components of the dissipative force given in Eq. (1), acting on the planets P_1 and P_2, respectively.

2.2. *The conservative model in the rotating frame*

We introduce now a *rotating frame* xOy, whose origin is the center of mass of the star S and the planet P_1 and the x axis is the line $S - P_1$ (see Fig. 1b). In this rotating frame the planet P_1 moves always on the x axis and the planet P_2 moves in the xOy plane. We still have four degrees of freedom, with variables (x_1, x_2, y_2, θ), where θ is the angle between the x axis and a fixed direction in inertial frame and defines the orientation of the rotating frame. The Lagrangian of the *conservative part* of the system, in the rotating frame, is

$$L = \frac{1}{2}(m_1 + m_2)\left\{q(\dot{x}_1^2 + x_1^2\dot{\theta}^2) + \frac{m_2}{m}\left[\dot{x}_2^2 + \dot{y}_2^2 + \dot{\theta}^2(x_2^2 + y_2^2) + 2\dot{\theta}(x_2\dot{y}_2 - \dot{x}_2 y_2)\right]\right\} - V, \tag{4}$$

where

$$V = -\frac{Gm_0m_1}{r_{01}} - \frac{Gm_0m_2}{r_{02}} - \frac{Gm_1m_2}{r_{12}}, \tag{5}$$

and

$$m = m_0 + m_1 + m_2,\ q = m_1/m_0. \tag{6}$$

We select the unit of mass in such a way that the total mass, m, of the system is equal to unity and the gravitational constant G, is also taken equal to unity:

$$m = m_0 + m_1 + m_2 = 1,\ G = 1. \tag{7}$$

The angle θ is ignorable and consequently the angular momentum $p_\theta = \partial L/\partial\dot{\theta}$, given by

$$p_\theta = (m_1+m_2)\left\{\dot{\theta}\left[qx_1^2+\frac{m_2}{m}(x_2^2+y_2^2)\right]+\frac{m_2}{m}(x_2\dot{y}_2-\dot{x}_2y_2)\right\}, \tag{8}$$

is constant. We can use now the angular momentum integral to reduce the number of degrees of freedom from four to three, by eliminating the ignorable angle θ ([Hadjidemetriou, 1975]). The new Lagrangian is the Ruthian function (see [Pars, 1965])

$$R = \frac{1}{2}\left\{q\dot{x}_1^2+\frac{m_2}{m}(\dot{x}_2^2+\dot{y}_2^2)-\frac{\left[\dfrac{p_\theta}{(m_1+m_2)}-\dfrac{m_2}{m}(x_2\dot{y}_2-\dot{x}_2y_2)\right]^2}{qx_1^2+\dfrac{m_2}{m}(x_2^2+y_2^2)}\right\}-V. \tag{9}$$

In this way we restrict our study in the rotating frame only, in the variables (x_1, x_2, y_2) and the six dimensional phase space $(x_1, x_2, y_2, \dot{x}_1, \dot{x}_2, \dot{y}_2)$. Note that p_θ appears as a fixed parameter in the Ruthian (9).

In the study of the evolution of the system we use the full system (Eqs. (3)), but transform the motion in the rotating frame xOy. In order to avoid unnecessary details in the computations and restrict the study to the general features only, we use the Poincaré map on the surface of section (Fig. 2a)

$$y_2 = 0,\ \dot{y}_2 > 0. \tag{10}$$

By the Poincaré map we reduce by one the dimension of the phase space, which is now the five dimensional space $(x_1, x_2, \dot{x}_1, \dot{x}_2, \dot{y}_2)$. In the following sections we shall present the results of the computations in projections in different coordinate planes or, equivalently, in projections in the orbital elements plane, mainly the eccentricity plane.

2.3. *Families of periodic orbits*

It is proved ([Hadjidemetriou, 1975], [Hadjidemetriou, 2002], [Beaugé et al., 2003]) that families of periodic orbits exist, *in a rotating frame*, in the planetary three body system mentioned above. There are two types of families of periodic orbits: (i) non resonant almost circular families of periodic orbits of the two planets and (ii) resonant families of periodic orbits, along which the eccentricities of the two planets increase, but the ratio of the frequencies of the planets in their motion around the star is almost constant (or, equivalently, the ratio of the semimajor axes is almost constant). The periodic orbits of the main families are symmetric with respect to the x axis, i.e. when $y_2 = 0$ it is $\dot{x}_1 = 0$, $\dot{x}_2 = 0$, which means that the non zero initial conditions of a symmetric periodic orbit are $(x_{10}, x_{20}, \dot{y}_{20})$. A family of symmetric periodic orbits is represented by a smooth curve in this space. Alternatively, a family of periodic orbits can be represented by a smooth curve in the space of the orbital elements (the eccentricities e_i, the semimajor axes a_i and the angles ω_i that define the orientation of the planetary orbits, for $i = 1, 2$). Note that for a symmetric periodic orbit the angles ω_i are either 0 or π. We remark that there exist also families of asymmetric periodic orbits, which bifurcate from the symmetric families ([Hadjidemetriou, 2006], [Voyatzis and Hadjidemetriou, 2006]).

In particular, the above mentioned circular family is symmetric. In Fig. 2b we present the circular family of periodic orbits (projection in the x_1x_2 plane), for the particular case of the masses $m_1 = 0.0008, m_2 = 0.0014, m_0 = 0.9978$ (for all other small masses the families are the same). Note that this family brakes at the 2/1 resonance and from that point on it continues as a family of symmetric 2/1 resonant periodic orbits, along which the eccentricities of the two planets increase. Along the circular family of non resonant, in general, periodic orbits, resonant orbits appear. The 4/1, 3/1 and 5/2 resonant orbits on the circular family are clearly seen. Families of elliptic periodic orbits bifurcate from the family of circular orbits at these resonances. For a full description see [Hadjidemetriou, 2006]. An important property of the circular family is that all orbits are stable, with the exception of a small region, at the 3/1 resonance, where instability appears ([Hadjidemetriou, 1982]).

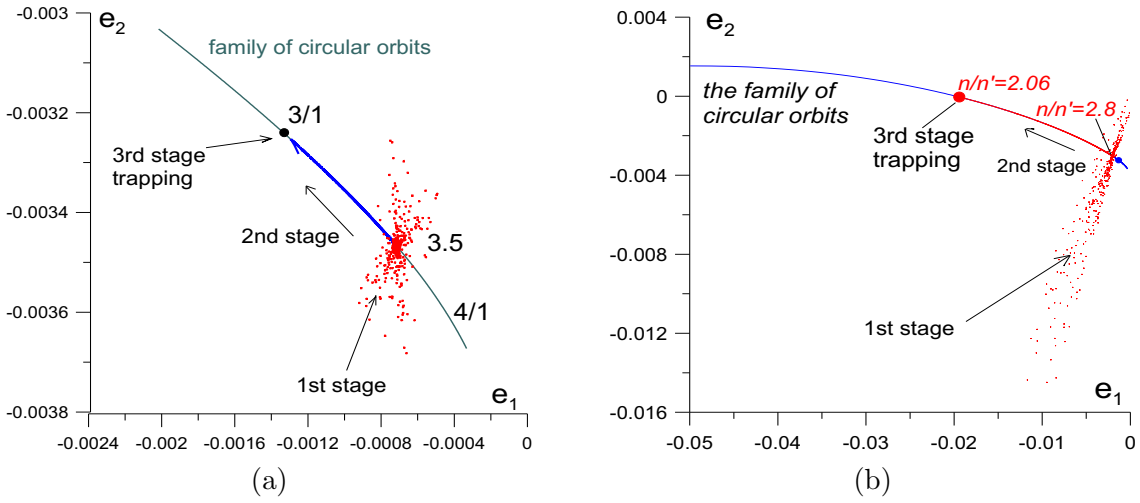

Fig. 3. (a) The evolution when the starting point corresponds to $n_1/n_2 > 3/1$. (b) The evolution when the starting point corresponds to $n_1/n_2 < 3/1$. The three stages of evolution are clearly seen. (We used the convention $e > 0$ when the planet is at perihelion and $e < 0$ when at aphelion).

3. Evolution of a non resonant orbit with large eccentricities

We study the long term evolution of a planetary system perturbed by a linear drag law (see Eqs. (3)), for different values of the masses and different initial conditions, starting from a non resonant system with large eccentricities. Since the system is dissipative, we expect the system to be trapped in some kind of attractor. The aim of this study is to find the different types of attractors that may appear. The computations are presented in the reduced three degrees of freedom system, in the rotating frame of Fig. 1b. All the computations were performed by the Bulirch - Stoer integration method, with an accuracy of 10^{-14}.

As mentioned before, the topology of the conservative Hamiltonian system critically depends on the families of periodic orbits. In particular, in our study, the family of circular orbits guides the evolution of the dissipative system, as we shall see in the next sections. We start with a non resonant system with large eccentricities ($e_1 = 0.20,\ e_2 = 0.20$) and a fixed value n_1/n_2 of the planetary frequencies. In all cases the evolution follows three distinct stages:

stage 1- attraction to a periodic orbit *on the circular family*, with almost the same value of n_1/n_2.
stage 2- motion *along* the circular family, with *decreasing* n_1/n_2.
stage 3- trapping in a resonance on the circular family.

There are different types of attractors at the third stage and we shall present typical examples for each particular case. A critical resonance on the circular family is the 3/1 resonance, because it is the only region where instability appears (for a proof see [Hadjidemetriou, 1982]). The evolution is different when we start with $n_1/n_2 > 3/1$ or with $n_1/n_2 < 3/1$, and for this reason these two cases will be studied separately. This is shown in Figs. 3a,b (for the case $m_1 = 0.0008,\ m_2 = 0.0014,\ m_0 = 0.9978$, but the evolution is similar in all cases).

The first stage of the evolution is *independent* of the initial eccentricities: all the orbits with the same value of n_1/n_2 and different eccentricities are attracted to the *same periodic orbit* on the circular family, with very small eccentricities, as it is shown in Fig. 4. This means that a large region in the eccentricity space is the basin of attraction of *the same* circular periodic orbit.

3.1. *Trapping in the 3:1 resonance*

In this section we present three typical cases. The starting point in all cases is $n_1/n_2 \approx 3.5$, which means that the attracting point on the circular family is *before* the unstable region at the 3/1 resonance (see Fig.

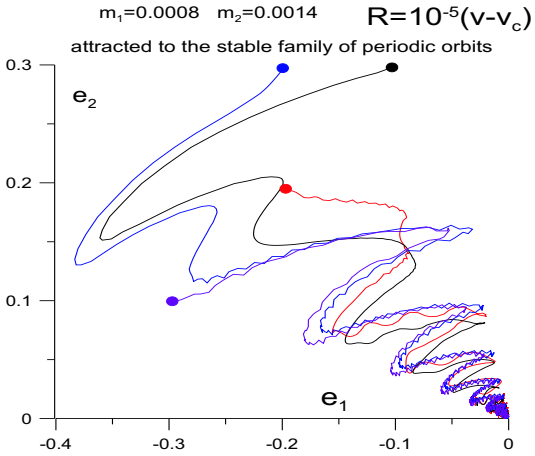

Fig. 4. All orbits in the eccentricity space, that start with different eccentricities and the same value for n_1/n_2 (in the present case $n_1/n_2 \approx 3.5$) are attracted to the same periodic orbit on the circular family, with almost the same ratio n_1/n_2.

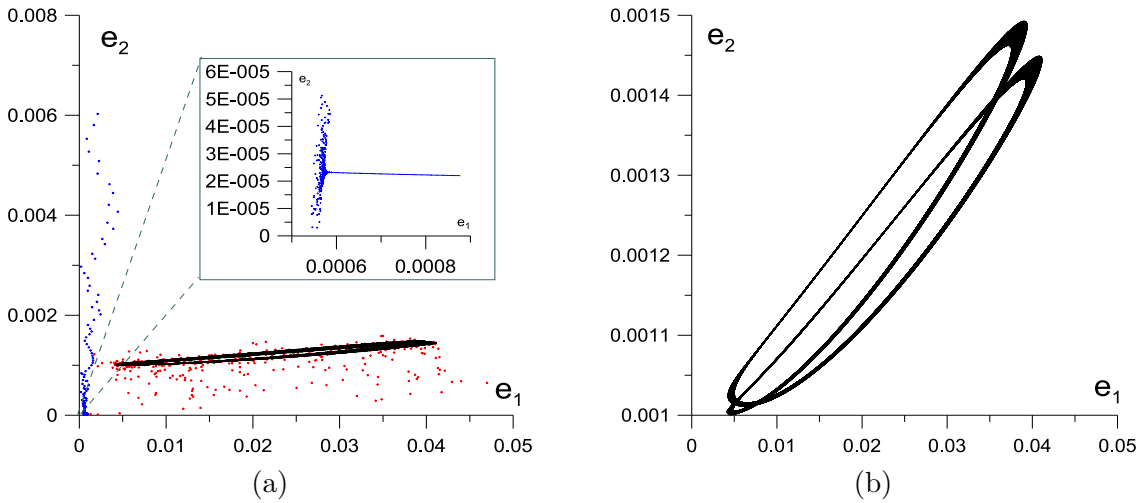

Fig. 5. The evolution of the system, with $m_1 = 0.00001$, $m_2 = 0.00100$, $e_1 = 0.20$, $e_2 = 0.20$ and $n_1/n_2 \approx 3.5$. (a) The three stages of the evolution: (1) The evolution from $e_1 = 0.20$, $e_2 = 0.20$ *toward* a periodic orbit on the circular family (blue). (2) The evolution *along* the family of circular orbits (box) until $n_1/n_2 = 3/1$. (3) The evolution close to the 3/1 resonance (red) and the final trapping, in the eccentricity space, to a limit cycle (black). (b) The final stage of the limit cycle.

3a). The lines of apsides of the planetary orbits coincide, with the perihelia in the same direction, and the two planets start at perihelion and aphelion, respectively. For the strength of the dissipation we used the value $n = 5$ in Eq. (1). In all cases, the first and the second stage (evolution toward the circular family and along the circular family) is the same. It is in the third stage that three different types of attractors appear (as shown in sections 3.1.1, 3.1.2 and 3.1.3).

3.1.1. *Case I: masses* $m_1 = 0.00001$, $m_2 = 0.00100$ *(*$m_1 < m_2$*)*

In this section we present the Poincaré map of the evolution of a system for $m_1 = 0.00001$, $m_2 = 0.00100$, starting with planetary eccentricities $e_1 = 0.20$, $e_2 = 0.20$ and mean motion ratio $n_1/n_2 \approx 3.5$. We present several projections in different coordinate planes, both in the orbital elements space (which gives a better physical understanding of the evolution) and in the coordinate space of the rotating frame, because the behavior could be very different. In Fig. 5 we present the three stages of evolution, in the eccentricity space. In panel (a) all three stages are present, and in panel (b) the final attractor is shown, which, *in this plane*, is a limit cycle. This means that the eccentricities of the two planets remain bounded, and close to

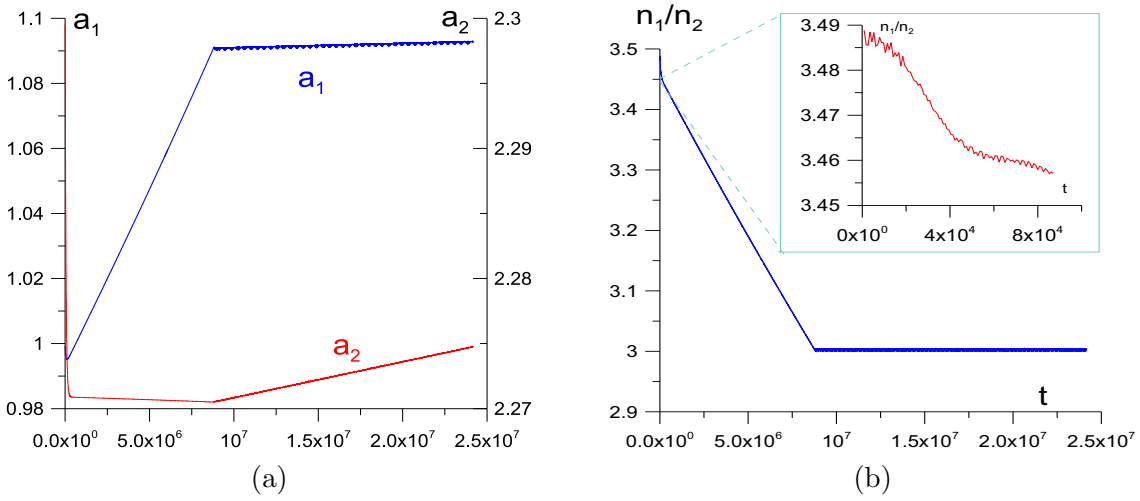

Fig. 6. (a) The evolution of the system with the parameters of Fig. 5, in the semimajor axes space. The first two stages of evolution (toward the family and along the family) and the third stage, after the trapping in the 3/1 resonance at $t \approx 10^7$, are presented. (b) The evolution of the ratio n_1/n_2. The trapping in the 3/1 resonance is clearly seen. The box shows the initial stage of the evolution.

zero. It is worth noting that the second stage is a *smooth* curve, which means that the system evolves *on* the circular family, until it meets the unstable region at the 3/1 resonance. Note also that, contrary to the second stage, irregular behavior appears both in the evolution *toward* the circular orbit (first stage) and the trapping in the 3/1 resonance (third stage), before the limit cycle in the eccentricity space.

In other coordinate planes the behavior is different at the third stage. The evolution of the semimajor axes is shown in Fig. 6a. The two semimajor axes follow a route along the circular family, but after the trapping in the 3/1 resonance they increase. This means that the size of the system increases, but the system remains similar to itself since a_1/a_2=constant. In Fig. 6b the evolution of the ratio n_1/n_2 is shown. The trapping in the 3/1 resonance is clearly seen. The chaotic behavior that appeared in the steps 1 and 3 is negligible in this projection.

We remark that the increase of the semimajor axes (and consequently of the size of the system) is due to the fact that the nonconservative force given by Eq. (1) is not purely dissipative. In fact, the differential rotation of the nebula corresponds to a forcing force, which is responsible for the change of the sign of the dissipation. This remark applies in all the cases that follow. The drag force given by Eq. (1) would be purely dissipative if the nebula did not rotate ($\vec{v}_c = 0$). In this case the semimajor axes decrease monotonically.

In Fig. 7a we present the evolution in the $x_1\dot{x}_1$ projection plane. The chaotic motion before the attraction to the circular family, the smooth evolution along the circular family and the irregular motion of the temporary trapping in the 3/1 resonance, before the final trapping in the limit cycle are clearly seen. The straight line that represents the motion along the family corresponds to $\dot{x}_1 = 0$, because the family of circular orbits is symmetric. This figure is similar to Fig. 5.

In Fig. 7b we present the projection in the x_1x_2 plane. Instead of the limit cycle of panel (a), we have the formation of a cylinder, whose radius is constant, but its size along the cylinder axis increases. This is a consequence of the proportional increase of the semimajor axes of both planets of the system, as shown in Fig. 6a.

Projection in different coordinate planes from those in Fig. 7 present the same evolution: limit cycle or cylinder. In particular, if the plane of projection includes the x_2 axis we have cylinder and in all other cases we have a limit cycle.

3.1.2. *Case II: masses* $m_1 = 0.00010$, $m_2 = 0.00010$ *(*$m_1 = m_2$*)*

In this section we repeat the work of section 3.1.1, for $m_1 = m_2 = 0.00010$, starting from $e_1 = 0.20$, $e_2 = 0.20$ and $n_1/n_2 \approx 3.5$. We find that the first and second stage are the same as in the previous case,

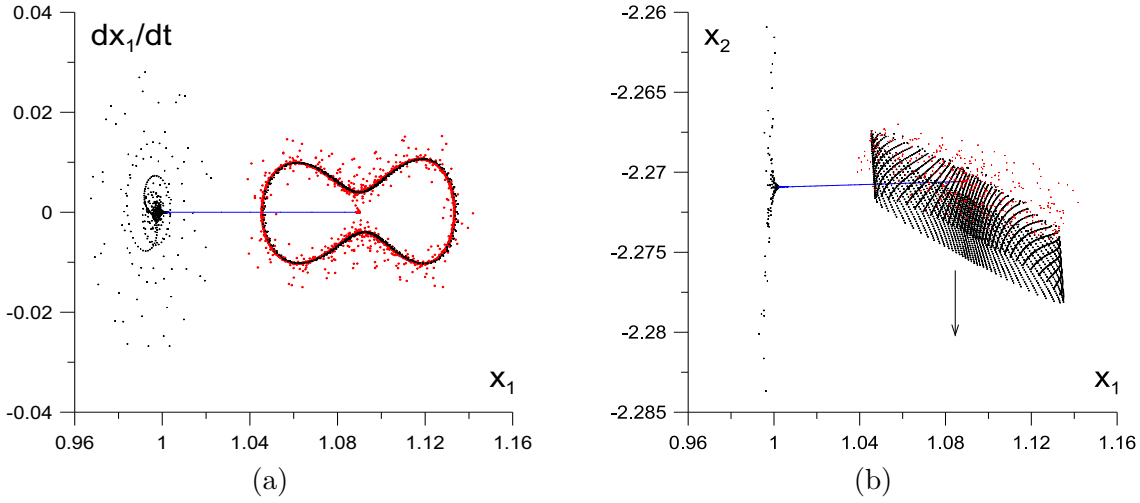

Fig. 7. The evolution of the system presented in Figs. 5 and 6, in the coordinate space. (a) Projection in the $x_1\dot{x}_1$ space. This evolution is similar to Fig. 5. Note the limit cycle in this space (black color). (b) Projection in the x_1x_2 plane. Instead of the limit cycle, we have now a cylinder.

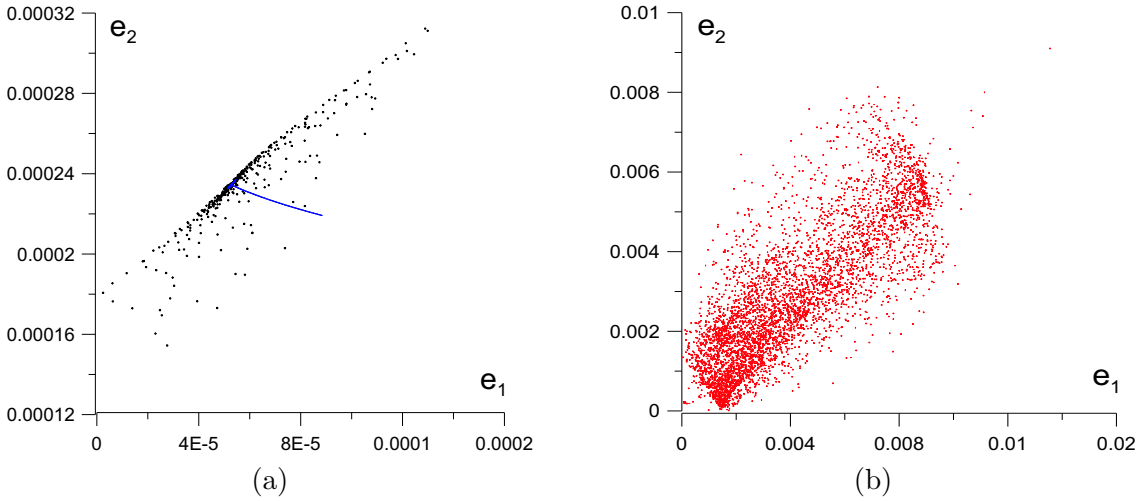

Fig. 8. The evolution of the system in the eccentricity space, with $m_1 = 0.00010$, $m_2 = 0.00010$, $e_1 = 0.20$, $e_2 = 0.20$ and $n_1/n_2 \approx 3.5$. (a) The evolution *toward* the circular family (black) and the evolution *along* the circular family (blue line). (b) The trapping in a bounded chaotic attractor at the 3/1 resonance.

but the third stage is different.

In Fig. 8a we present the first two stages of evolution in the eccentricity space: motion toward the circular family (black) following a chaotic route and the smooth motion along the family (blue line). In Fig. 8b we present the third stage, where the system is trapped in a bounded chaotic attractor, implying that the eccentricities are trapped in very small values.

In Fig. 9a we present the evolution in the semimajor axes space. The two semimajor axes follow a smooth route along the circular family, but after the trapping in the 3/1 resonance they increase. This means that the size of the system increases, but the system remains similar to itself (a_1/a_2 =constant). In Fig. 9b the evolution of the ratio n_1/n_2 is shown. The trapping in the 3/1 resonance is clearly seen. The chaotic behavior is negligible in this projection.

In Fig. 10 we present the evolution in projection in coordinate planes of the rotating frame. This Figure is similar to Fig. 8. In Fig. 10a we have the projection in the $x_1\dot{x}_1$ plane. The chaotic motion before the attraction to the circular family, the evolution along the circular family and the chaotic motion of the final

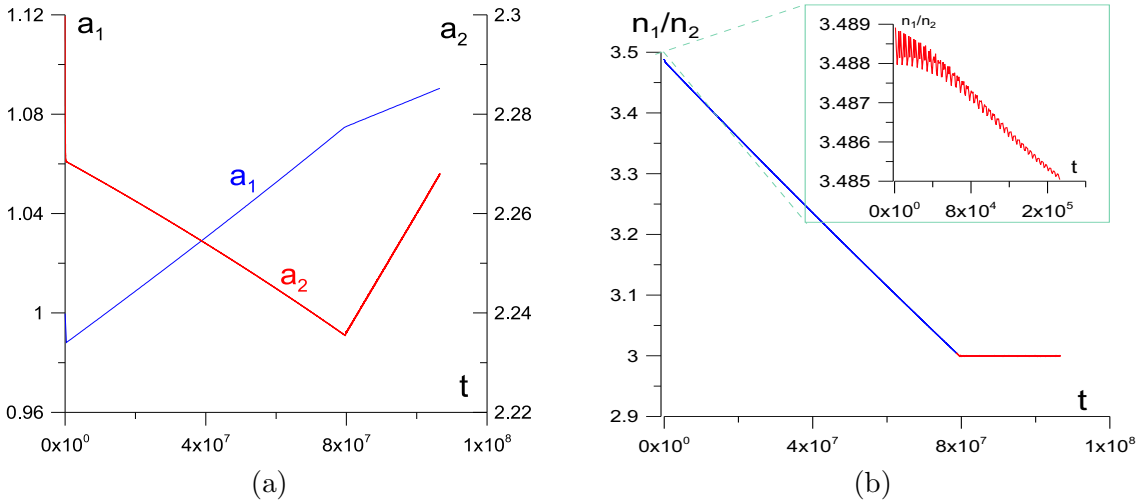

(a) (b)

Fig. 9. (a) The evolution of the semimajor axes. After the trapping in the chaotic attractor at the 3/1 resonance, at $t \approx 8\times10^7$, the values of both a_1, a_2 increase. (b) The evolution of the ratio n_1/n_2. The trapping in the 3/1 resonance is clearly seen. The box shows the initial stage of the evolution.

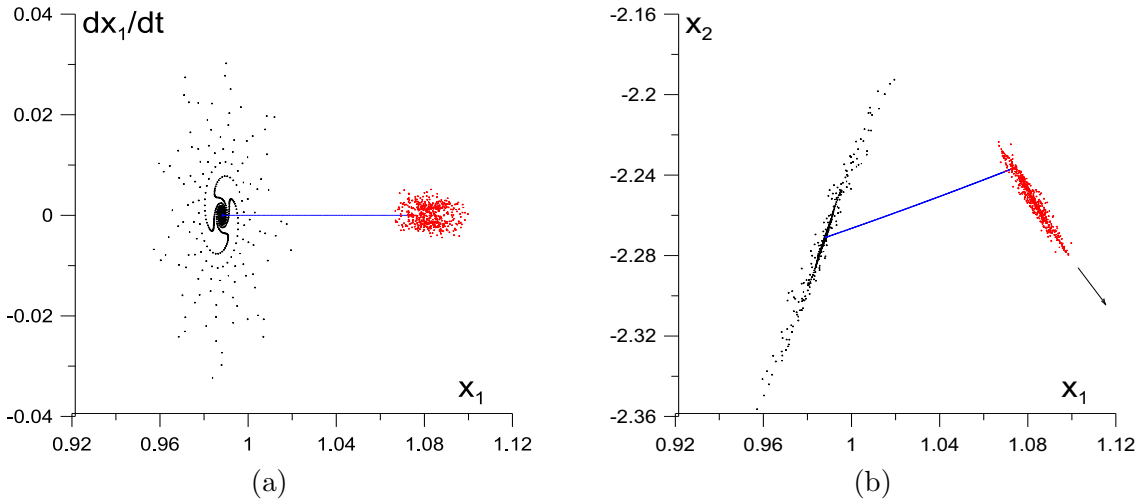

(a) (b)

Fig. 10. The evolution of the system presented in Figs. 8 and 9 in the coordinate space of the Poincaré map. (a) Projection in the $x_1\dot{x}_1$ space. (b) Projection in the x_1x_2 plane. This evolution is similar to Fig. 8.

trapping in the 3/1 resonance are presented. The straight line that represents the motion along the family corresponds to $\dot{x}_1 = 0$, because the family of circular orbits is symmetric (see also Fig. 7a).

In Fig. 10b we present the projection in the x_1x_2 plane. This is similar to the evolution of panel (a), but now the size of the chaotic attractor of the third stage (red) increases. This is a consequence of the increase of the size of the system for $t > 8 \times 10^7$, as shown in Fig. 9a for the evolution of the semimajor axes.

3.1.3. *Case III: masses* $m_1 = 0.00100$, $m_2 = 0.00001$ $(m_1 > m_2)$

In this section we repeat the work of sections 3.1.1 and 3.1.2, for $m_1 = 0.00100$, $m_2 = 0.00001$, $e_1 = 0.20$, $e_2 = 0.20$ and $n_1/n_2 \approx 3.5$. Projections in different coordinate planes, both in the orbital elements space and the coordinate space of the rotating frame are presented. The first and second stage is the same as in the previous cases, but the third stage is different from the two previous cases.

In Fig. 11a we present the first two stages of the evolution (motion toward the circular family and

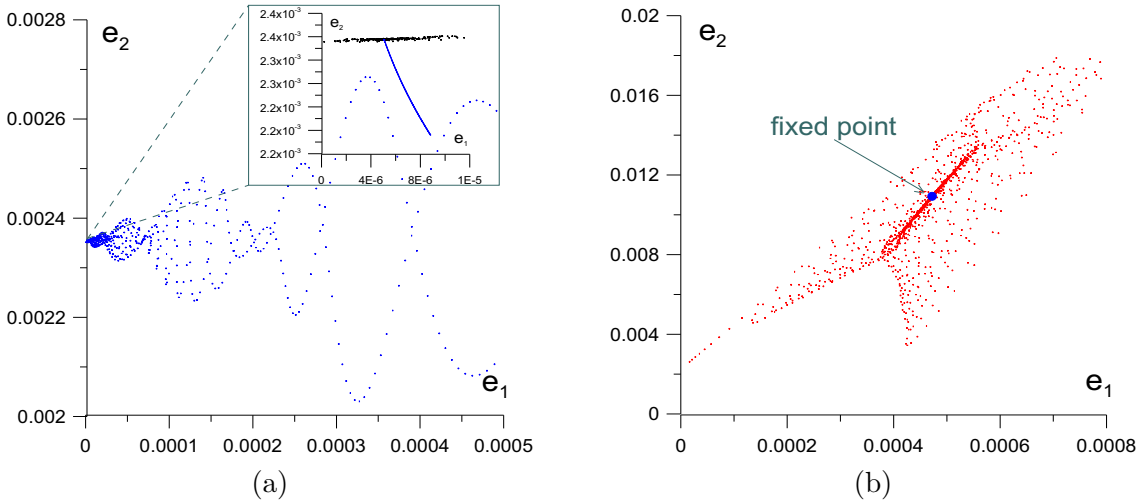

Fig. 11. The evolution of the system, with $m_1 = 0.00100$, $m_2 = 0.00001$, $e_1 = 0.20$, $e_2 = 0.20$ and $n_1/n_2 \approx 3.5$ in the eccentricity space. (a) The evolution *toward* the circular family and the evolution *along* the circular family (box, blue line). (b) The temporary trapping in a chaotic attractor (red) and the final trapping in a *fixed point*.

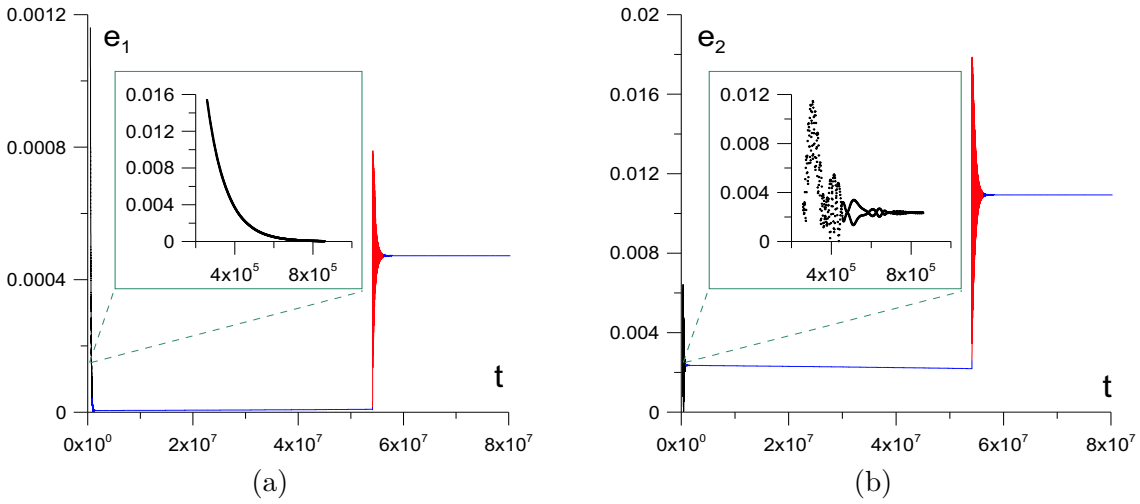

Fig. 12. The evolution of the eccentricities and the final trapping in fixed eccentricities. (a) The evolution of e_1: Motion toward the circular family (box), the motion along the circular family (blue line), the temporary trapping in the chaotic attractor (red) and the final trapping in a fixed value (blue line). (b)The same as in panel (a), for e_2.

motion along the circular family). This behavior is the same as in the previous two cases, in sections 3.1.1. and 3.1.2. The third stage however, presented in Fig. 11b is different. There is a *temporary* trapping in a chaotic attractor, at the 3/1 resonance, but the system is finally attracted to a *fixed point*, in the eccentricity space. This is clearly seen in Fig. 12, where the evolution of the eccentricities is shown. The trapping of e_1 and e_2 in fixed values, close to zero, is evident.

In Fig. 13a we present the evolution in the semimajor axes space. The two semimajor axes follow a smooth route along the circular family, but after the trapping in the 3/1 resonance they increase. This means that the size of the system increases, but the system remains similar to itself, as we mentioned in the previous cases. In Fig. 13b the evolution of the ratio n_1/n_2 is shown and the trapping in the 3/1 is clearly seen.

In Fig. 14a we present the projection of the trajectory in the $x_1\dot{x}_1$ plane and in Fig. 14b the projection in the x_1x_2 plane. In both cases we observe the irregular motion before the attraction to the circular family (black), the evolution along the circular family (blue line), the temporary chaotic motion (red) and the

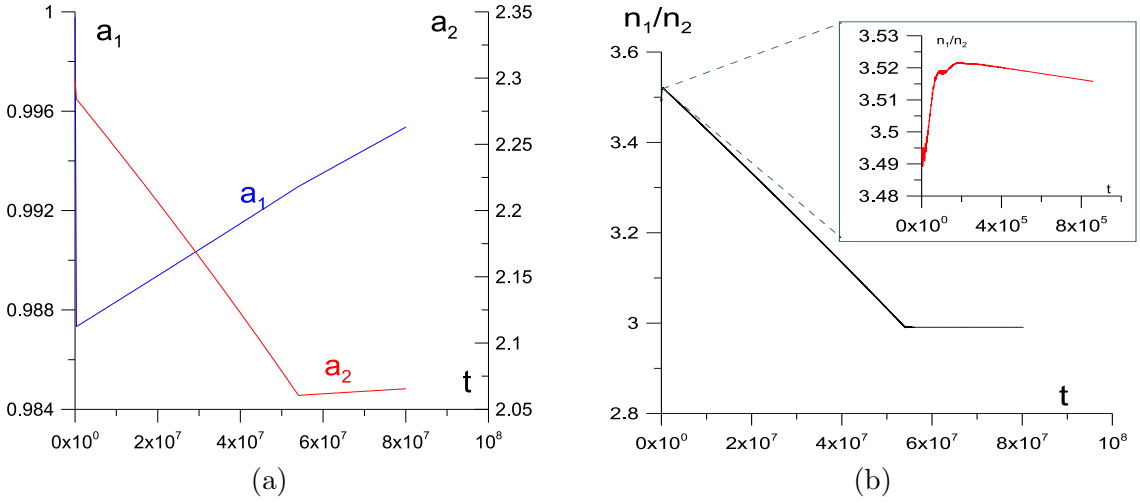

Fig. 13. (a) The evolution of the semimajor axes. After the trapping in the chaotic attractor at the 3/1 resonance, at $t \approx 5.3 \times 10^7$, the values of both a_1, a_2 increase. (b) The evolution of the ratio n_1/n_2. The trapping in the 3/1 resonance is clearly seen. The box shows the evolution toward the circular family.

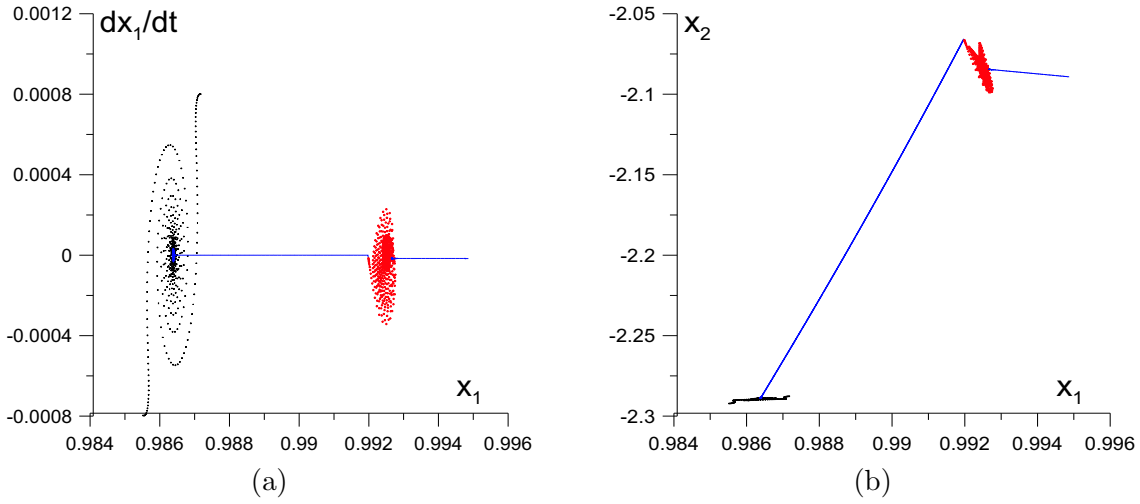

Fig. 14. The evolution of the system presented in Figs. 11, 12 and 13, in the coordinate space of the Poincaré map. The four stages of evolution mentioned in Fig. 12 are clearly seen. (a) Projection in the $x_1\dot{x}_1$ plane. (b) Projection in the x_1x_2 plane.

final trapping in an orbit with fixed eccentricities but increasing in size, remaining similar to itself (blue line). This latter straight line corresponds to the fixed point of Fig. 13a.

The results presented above were obtained for $n = 5$ and specific values of the masses. Different values of n ($n > 5$), corresponding to different dissipation strengths and different planetary masses, give one of the three types of evolution described in the previous subsections, as we have checked by many numerical computations. Consequently, a slow decrease of the strength of the drag law, in the process of the evolution, does not affect the qualitative results, but only the time rate of the evolution. We checked this by assuming in some computations coefficients that decrease on time.

3.2. *Trapping in the 2:1 resonance*

In section 3.1 we studied the evolution of a non resonant system that started with a frequency ratio n_1/n_2 of the two planets larger than 3/1. Since, as we explained before, during the first stage of the evolution (motion of the system to a periodic orbit of the circular family) the value of n_1/n_2 remains almost constant, the system reaches the circular family at an orbit *before* the unstable region at the 3/1 resonance. So, as

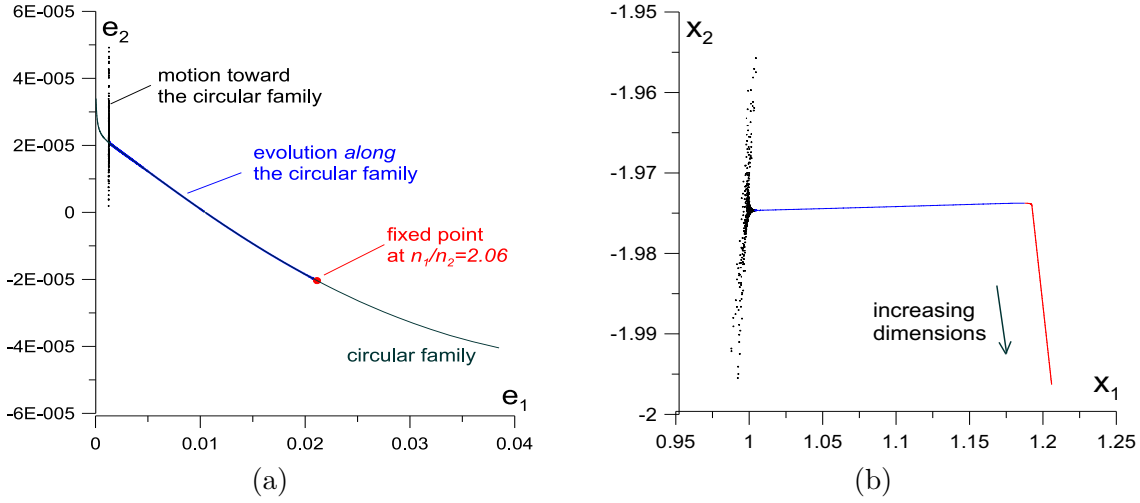

Fig. 15. The evolution of the system, with $m_1 = 0.00001$, $m_2 = 0.00100$, $e_1 = 0.20$, $e_2 = 0.20$ and $n_1/n_2 \approx 2.8$. (a) The three stages of the evolution: (1) The evolution from $e_1 = 0.20$, $e_2 = 0.20$ *toward* a periodic orbit on the circular family (black). (2) The evolution *along* the family of circular orbits until $n_1/n_2 \approx 2/1$ (blue). (3) The final trapping, in the eccentricity space, to a fixed point (red). The family of circular orbits (green) is also presented. (b) The same evolution as in panel (a), in the x_1x_2 plane. The size after the trapping close to the 2/1 resonance increases, due to the increase of the semimajor axes (Fig. 16a).

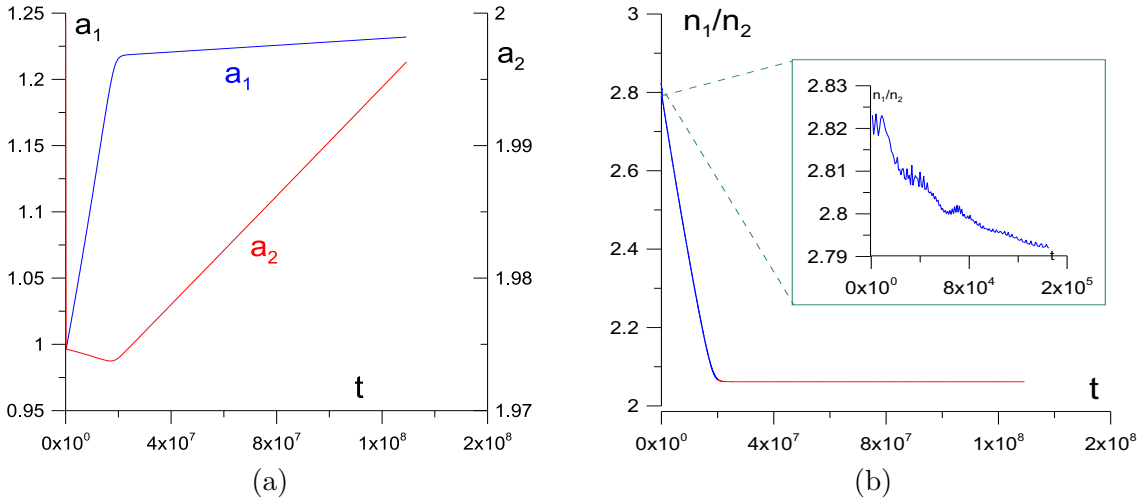

Fig. 16. (a) The evolution of the semimajor axes. After the trapping in the chaotic attractor close to the 2/1 resonance, at about $t = 2 \times 10^7$, the values of both a_1, a_2 increase. (b) The evolution of the ratio n_1/n_2. The trapping close to the 2/1 resonance is clearly seen. The box shows the evolution toward the circular family.

the system evolves along the family with decreasing n_1/n_2 (second stage), it meets the unstable region and is trapped there. In the present section we study the case where the system starts *after* the 3/1 resonance, i.e $n_1/n_2 < 3/1$. So, as the system evolves along the circular family, it does not encounter any unstable region, and we have a different kind of evolution.

We present in the following a typical example. The initial ratio of the planetary frequencies is taken equal to $n_1/n_2 \approx 2.8$. All other cases (different masses and different values of n) have the same behavior.

In Fig. 15a we present the evolution in the eccentricity space. After the chaotic motion toward the circular family with almost the same ratio n_1/n_2, the system smoothly moves *along* the circular family and is finally trapped in a fixed point on the family of circular orbits, in the eccentricity space, close to the 2/1 resonance. In Fig. 15b we present the same evolution in the x_1x_2 coordinate plane. The motion along the circular family is evident, but now the size increases because the semimajor axes increase (see Fig. 16).

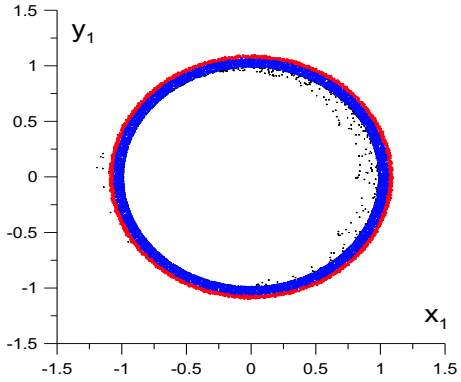

Fig. 17. The evolution of the system, with $m_1 = 0.00001$, $m_2 = 0.00100$, $e_1 = 0.20$, $e_2 = 0.20$ and $n_1/n_2 \approx 3.5$, in the $x_1 y_1$ plane of the *inertial* system. The three colors, black, blue, red, correspond to the three stages of evolution, respectively.

In Fig. 16a the evolution of the semimajor axes is presented. After the trapping close to the 2/1 resonance, the size of the system increases, while the system remains similar to itself. In Fig. 16b the evolution of the ratio n_1/n_2 is presented showing the resonance trapping in the value $n_1/n_2 \approx 2.06$.

In the present case, $n_1/n_2 < 3$, the evolution for different values of the masses and the value of n is always the same: trapping in a fixed point on the circular family close to the 2/1 resonance. The behavior is also the same when the drag force decreases slowly as we mentioned in section 3.1.

We also note that if we start with $n_1/n_2 > 3/1$, as in section 3.1, but with a stronger drag force, taking $n = 4$ or $n = 3$ in Eq. (1), the system does not stop at the 3/1 unstable region, as it moves along the circular family, but continues until the 2/1 resonance and is trapped in a fixed point on the circular family, close to the 2/1 resonance. This behavior is the same as the one shown in section 3.2, Fig. 15a.

4. Conclusion

The important conclusion of this work is that the evolution of the non conservative system is *guided* by the families of periodic orbits of the *conservative* part. These families are attractors of the complete system. Different types of attractors appear, depending on the initial conditions and the parameters of the system. The fine structure and the details of the evolution are evident only in the reduced three degrees of freedom system (or, equivalently, in the orbital elements space). The projection of the Poincaré map of the evolution of the system in a coordinate plane of the *inertial frame* does not show anything interesting, as is seen for example in Fig. 17.

We restricted the present study to initial non resonant configurations, i.e. the ratio n_1/n_2 of the planetary frequencies is not rational (equal to p/q, with small values for p, q) and large eccentricities. In all cases there was a rapid attraction to a periodic orbit on the *circular family* of periodic orbits, with almost the same value of n_1/n_2. The system however does not stop there, but evolves *along* the circular family, with decreasing n_1/n_2.

If we start with $n_1/n_2 > 3/1$ and $n \geq 5$, the system arrives at first on a periodic orbit of the circular family *before* the unstable region at the 3/1 resonance and moves thereafter smoothly along the family until it meets the unstable region at the 3/1 resonance (we remind that this is the only unstable region on the circular family, up to the 2/1 resonance). At this region, three types of attractors appear depending on the values of the parameters. Typical examples are given in sections 3.1.1, 3.1.2 and 3.1.3, respectively. An important feature of the attractors is that they show different properties in the projections in different coordinate planes. In the eccentricity space we may have a limit cycle after a temporary trapping in an irregular motion (section 3.1.1), a bounded chaotic attractor (section 3.1.2) or a fixed point, after a temporary trapping in an irregular motion (section 3.1.3). In other coordinate planes however, for example the plane of the semimajor axes, we have an increase of the size of the system, but the system remains similar to itself, since it is finally trapped in the 3/1 resonance. This feature is also evident in the projections

in different coordinate planes of the rotating frame.

If we start with $n_1/n_2 < 3/1$, the system arrives at first on a periodic orbit of the circular family *after* the unstable region at the 3/1 resonance and moves thereafter smoothly along the family and is finally trapped in a fixed point (in the eccentricity space) close to the 2/1 resonance. In this case (section 3.2), the evolution is the same for all parameters. The evolution of the semimajor axes and the size of the system are similar to the case $n_1/n_2 > 3/1$.

We remark that if the strength of the drag force is quite large ($n < 5$) and we start with $n_1/n_2 > 3/1$, the system is not trapped in the unstable 3/1 resonance, as it evolves along the circular family, but continues until the 2/1 resonance and is trapped in a fixed point in the eccentricity space, as in the case of section 3.2.

It is worth noting that in all cases the family of periodic orbits behaves as a "river", along which the system flows, until it meets a major resonance. The importance of resonances is clear, because it is at certain resonances that instabilities appear, which affect the topology of the phase space.

The strength of the dissipative force, determined by the value of n in Eq. (1), does not affect the evolution of the system, but only the time rate of the evolution. The same types of evolution, presented in section 3, appear for all values of n and of the planetary masses. This implies that a slow decrease of the dissipation strength does not affect the evolution, as we checked by several numerical computations. Of course, if the drag force decreases to zero, due to a slow decrease of the density of the protoplanetary nebula, the final configuration may be an intermediate state of the evolution that we presented.

As stated before, the present work was restricted to the particular non conservative force of Eq. (1). Different non conservative laws have different types of evolution. Also, for starting conditions close to families of *resonant* periodic orbits, the trajectories have different types of evolution. In all cases however, it is the families of periodic orbits of the conservative part that guide the evolution of the system.

References

Beaugé, C., Ferraz-Mello, S. [1993] "Resonance trapping in the primordial solar nebula: the case of Stokes drag dissipation", Icarus **103**, 301–318.

Beaugé, C., Ferraz-Mello, S. and Michtchenko, T. [2003] "Extrasolar Planets in Mean-Motion Resonance: Apses Alignment and Asymmetric Stationary Solutions", ApJ **593**, 1124–1133.

Beaugé C., Ferraz-Mello S., Michtchenko T.A. [2006] "Planetary Migration and Extrasolar Planets in the 2/1 Mean-motion Resonance", MNRAS **365**, 1160-1170.

Crouch, P. E., and van der Schaft, A. J. [1987], "Variational and Hamiltonian Control Systems", Springer-Verlag

Ferraz-Mello, S., Beaugé, C. and Michtchenko T.A. [2003] "Evolution of migrating planet pairs in resonance", CM&DA **87**, 99–112.

Gomes R.S.[1996] "The effect of Nonconservative forces on resonance lock: stability and instability", Icarus **115**, 47–59.

Hadjidemetriou J.D. [1975] "The continuation of periodic orbits from the restricted to the general three-body problem", CM&DA **12**, 155–174.

Hadjidemetriou, J.D. [1982] "On the Relation between Resonance and Instability in Planetary Systems", CM&DA 27, 305-322.

Hadjidemetriou, J.D. [2001]"Resonant periodic motion and the stability of extrasolar planetary systems", CM&DA **83**, 141–154.

Hadjidemetriou, J.D. [2006] "Symmetric and Asymmetric Librations in Extrasolar Planetary Systems: A global view", CM&DA **95**, 225–244.

Hadjidemetriou, J.D. and Voyatzis, G. [2010] "On the dynamics of extrasolar planetary systems under dissipation: Migration of planets", CM&DA **107**, 3–19.

Haghighipour N. [1999] "Dynamical friction and resonance trapping in planetary systems", MNRAS **304**, 185–194.

Michtchenko T.A., Beaugé C., Ferraz-Mello S. [2006], "Stationary Orbits in Resonant Extrasolar Planetary Systems", CM&DA **94**, 381–397.

Morbidelli A., Tsiganis K., Grida A., Levison H.F., Gomes R. [2007] "Dynamics of the giant planets of the solar system in the gaseous protoplanetary disk and their relation to the current orbital architecture", Astron. J. **134**, 1790-1798.

Nelson R.P., Papaloizou J.C.B. [2003a] "The interaction of a giant planet with a disk with MHD turbulence - I. The initial turbulent disc models", MNRAS **339**, 983–992

Nelson R.P., Papaloizou J.C.B. [2003b] "The interaction of a giant planet with a disk with MHD turbulence - II. The interaction of the planet with the disk", MNRAS **339**, 993–1005

Papaloizou J.C.B. [2003] "Disk planet interactions: migration and resonances in extrasolar systems", CM&DA **87**, 53–83.

Pars, L.S. [1965] "A Treatise on Anamytical Dynamics", Heinemann, London, paragr. 10.1, 22.

Voyatzis, G. and Hadjidemetriou , J.D. [2006]: " Symmetric and asymmetric 3:1 resonant periodic orbits: An application to the 55Cnc extra-solar system", CM&DA **95**, 259-271.